Solar and Stellar Magnetic Fields: Origins and Manifestations
Proceedings IAU Symposium No. 354, 2019
A. Kosovichev, K. Strassmeier & M. Jardine, ed.
doi:10.1017/S1743921320000186

Diagnosing chromospheric magnetic field through simultaneous spectropolarimetry in H α and Ca II 854.2 nm

K. Nagaraju[1], K. Sankarasubramanian[2] and K. E. Rangarajan[1]

[1]Indian Institute of Astrophysics, Sarjapur Road, Bengaluru, India
email: nagarajuk@iiap.res.in; rangaraj@iiap.res.in

[2]URSC & ISRO, Vimanapura, Bengaluru, India
email: sankark@ursc.isro.gov.in

Abstract. Measurement of magnetic field in this layer is challenging both from point of view of observations and interpretation of the data. We present in this work about spectropolarimetric observations of a pore, simultaneously in Ca II (CaIR) at 854.2 nm (CaIR) and H α (656.28 nm). The observed region includes a small scale energetic event (SSEE) taking place in the region between the pore and the region which show opposite polarity to that of pore at the photosphere. The energetic event appears to be a progressive reconnection event as shown by the time evolution of the intensity profiles. Closer examination of the intensity profiles from the downflow regions suggest that the height of formation of CaIR is higher than that of Hi α, contrary to the current understanding about their height of formation. Preliminary results on the inversion of Stokes-I and V profiles of CaIR are also presented.

Keywords. Photosphere: Magnetic field, Chromosphere: Magnetic field, Multi-line-Spectropolarimetry

1. Introduction

Accurate knowledge of magnetic field at multiple heights in the solar atmosphere is of paramount importance to understand the various dynamics such as energy transportation and dissipation, energetic events of various spatial and energy scales, wave-dynamics, just to name a few. Measurement of magnetic field at the photosphere is carried out more or less on routine basis. But at the higher layers it is much more challenging due to weak polarimetric signals in the spectral lines because of the weaker magnetic fields and the inference of magnetic field from the observed spectrum requires taking into account the NLTE effects. Inspite of this there has been a significant progress towards chromospheric magnetic field measurements in the recent past (Lagg *et al.* 2017). Some of the most widely used spectral lines for inferring chromospheric magnetic field are CaIR and He I 10830 lines (Lagg *et al.* 2017) while efforts on exploring the diagnostic capability of other spectral lines is still going on. However, each of these lines have their own strengths and limitations under certain conditions. The He I samples mostly upper chromospheric layers and it's formation depends on the coronal EUV emission (Andretta & Jones 1997). On the other hand CaIR line gets completely ionized during flares (Kerr *et al.* 2016; Kuridze *et al.* 2018; Bjørgen *et al.* 2019). In order to probe wide range of dynamics those take place in the chromosphere, multi-line spectropolarimetry is needed. In this context H α may play an important role in probing chromospheric magnetic field as it's ubiquitously present in the wide variety of chromospheric plasma conditions such as quiet sun, active regions(Rutten 2007, 2008) and flaring regions (Bjørgen *et al.* 2019).

Inspite of its ubiquitous presence H α has been rarely used for probing chromospheric magnetic field. To mention a few, Abdusamatov & Karat (1971); Balasubramaniam *et al.* (2004); Hanaoka (2005); Nagaraju *et al.* (2008) have presented chromospheric magnetic field measurements through H α spectropolarimetry. One of the reasons for rarely using this line for magnetic field measurements is interpreting the observations is notoriously difficult. For instance Socas-Navarro & Uitenbroek 2004 have shown through numerical simulations that H α Stokes-V is sensitive to photospheric magnetic field in quiet sun model while its temperature sensitivity is in chromosphere. However, Leenaarts *et al.* (2012) have shown through numerical simulation that solving 3D radiative transfer equation is essential to model H α line and shown that it has a good sensitivity to chromospheric magnetic field. Very recently Bjørgen *et al.* (2019) have shown again through simulation that flare ribbons are seen in all chromospheric lines including H α but least visible in CaIR.

Hence exploring diagnostic capability of H α is important. In this context we compare in this paper about the simultaneous spectropolarimetric observations in CaIR and H α. The comparison is done above pore, opposite polarity region and SSEE. Though the observations were of full Stokes polarimetry, we present only Stokes-I and V profiles because Stokes-Q and U signals are weak or negligible compared to the noise level.

2. Observations and Data reduction

Simultaneous spectropolarimetric observations in H α and CaIR were carried out using the Spectropolarimeter for Infrared and Optical Regions (SPINOR: Socas-Navarro *et al.* 2006) at the Dunn Solar Telescope, National Solar Observatory, Sunspot, New Mexico. The spatial sampling in scan and slit directions is 0.3″/pixel on the Sarnoff camera used for recording the H α spectrum. The spectral sampling is 22.45 mÅ/pixel and the spectral resolution is 32.18 mÅ. For CaIR region the spatial sampling is same as that of H α while the spectral sampling is 33.73 mÅand the spectral resolution is 49.17 mÅ.

The region of observations on the sun was around a small pore (Fig. 1). The cosine of the heliocentric angle μ is 0.536. Though the observations were carried out on four successive days from 4 through 7 December 2008, only a few scans obtained on 4 December are with a reasonably good seeing. Four scans of of 20 slit positions with a corresponding spatial extent of 6″ recorded at 15:35, 15:42, 15:57 and 16:08 UT are considered for analysis. Each raster map took about 3 minutes to scan. The noise level in the Stokes profiles is in the order $10^{-3}I_c$ (I_c is the continnum intensity).

The data were subjected to bias and flat corrections. The data were corrected for polarimeter response using the calibration data obtained on the same day of observation. To correct for the telescope induced cross-talks we have used the telescope calibration data obtained during May 2005. Since it is a very old calibration the cross-talk among Stokes parameters was not corrected very well. To correct for these residual cross-talks we have applied scatter plot method (Sanchez Almeida & Lites 1992; Schlichenmaier & Collados 2002). Only the cross-talk from Stokes V to Stokes Q and U is corrected as the amplitude of former is always greater than the amplitudes of later ones. The cross-talk from intensity to polarisation is corrected by assuming the continuum to be non-polarized. Estimation of stray-light factor was done by comparing disc center Stokes-I profiles with that of atlas spectrum (FTS). The estimated straylight was about 18%. Nearby quiet sun profile was used as profile function for the straylight.

The observing period covers a small scale energetic event (SSEE). The raster maps of the observed region is shown in Fig. 1. The first map in this figure corresponds to the continuum close to H α, the second, third and fourth maps correspond to the line core intensities of Fe I at 656.922 nm, H α and CaIR, respectively and the fifth, the sixth and the seventh maps correspond to the respective Stokes-V amplitudes. The region of SSEE

https://doi.org/10.1017/S1743921320000186 Published online by Cambridge University Press

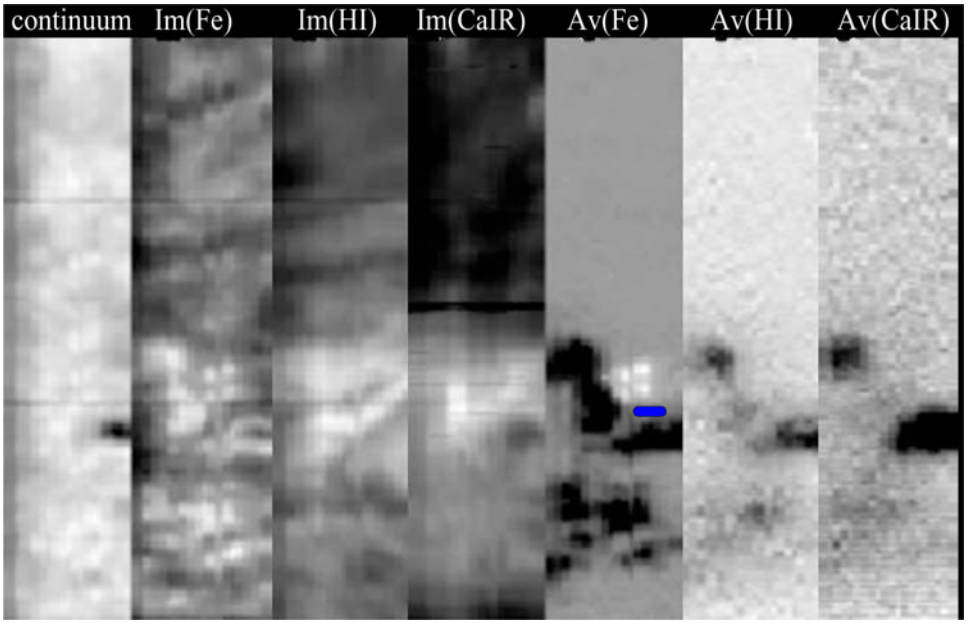

Figure 1. Raster maps of the observed region. The left most raster map corresponds to the continuum (close to H α) followed by the line core intensity images of Fe I at 656.922 nm, H α and CaIR, respectively and the last three column correspond to the respective Stokes-V amplitudes.

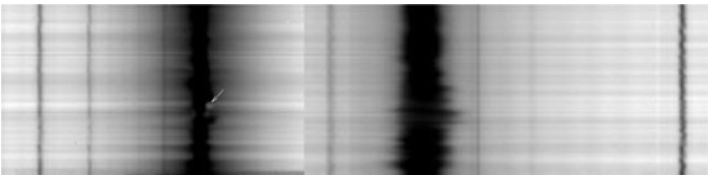

Figure 2. Stokes-I spectral images of H α and CaIR corresponding to a SSEE (as indicated by an arrow on the CaIR spectrum).

is indicated by a blue rectangular box placed on the Stokes-V amplitude map of Fe I line at 656.922 nm. Also seen in this map is the region of magnetic field which is opposite to that of pore. Though it is visible only in the photospheric line, henceforth we refer this region as the opposite polarity region.

Sample spectral images of CaIR (left panel) and H α (the right panel) corresponding to a slit position above SSEE are shown in Fig. 2. The SSEE is indicated by an arrow in this figure shows up as a mustache structure in the CaIR spectrum, typical of Ellerman bomb event (Ellerman 1917). However, there's no signature EB in the H α spectral image. The time evolution of intensity profiles as shown Fig. 3 suggest that SSEE is a progressive reconnection event smilar to that of flaring arch filament (Vissers *et al.* 2015). Initially emission in the wings of CaIR is observed indicating that the heating taking place in the lower atmospheric layers. The H α shows evelated intensity profiles. Towards the end of our observations, CaIR line core goes in to emission and H α line gets further elevated due to the heating taking place in the region. The magnetic field geometry associated with the SSEE seems to have a simple configuration with the newly emerged opposite polarity fields reconnecting with the canopy fields of the pore.

In the beginning of the SSEE the region shows strong downflows. Sample profiles are shown in Fig. 4. The left and the right panels in this figure show CaIR and H α intensity

https://doi.org/10.1017/S1743921320000186 Published online by Cambridge University Press

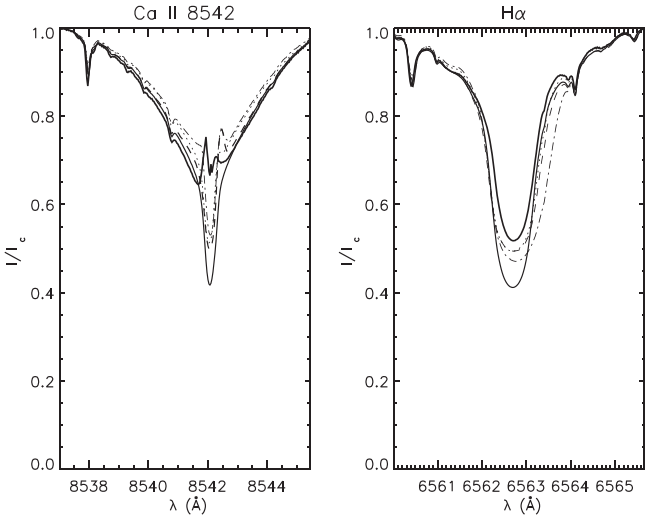

Figure 3. Stokes-I profiles of H α and CaIR corresponding to the SSEE. The thin solid curves correspond to a quiet sun region, The dotted, dashed, dash-dotted and thick solid curves correspond to the spectra observed at 15:35, 15:42, 15:57 and 16:08 UT, on 4 December, 2008, respectively.

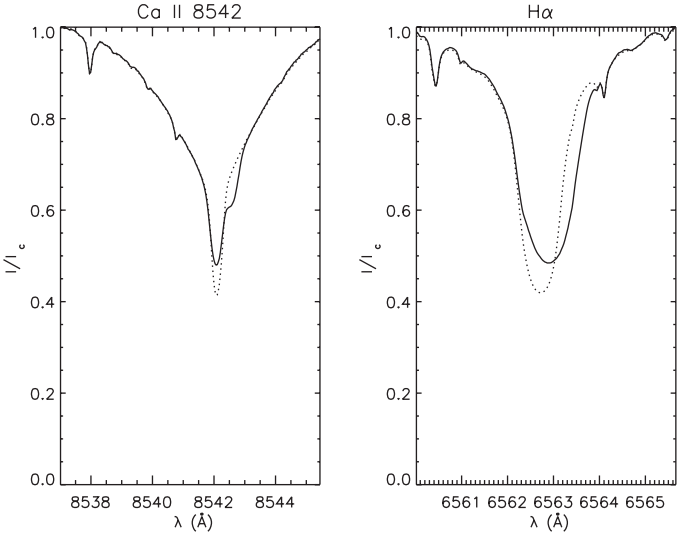

Figure 4. Stokes-I profiles of CaIR (the left panel) and H α (the right panel) showing downflows during the reconnection event.

profiles (the solid curves), respectively. The dotted curves correspond to the respective quiet sun profiles. While the CaIR shows redshift away from the line core, H α shows redshift including its line core. This possibly indicates that the height of formation of H α is lower than that of the CaIR. This is contrary to the current understanding that height of formation of CaIR is very close to that of H α or slighty below.

Sample Stokes-I (the top row) and V (the bottom row) profiles of CaIR (the panels on the left column) and H α (the panels on the right column) are shown in Fig. 5 above the opposite polarity region (see Stokes-V amplitude map of Fe I in Fig. 1). The Stokes-V profile of H α has the polarity opposite to that of Fe I line at 656.922 nm which forms at

https://doi.org/10.1017/S1743921320000186 Published online by Cambridge University Press

Table 1. Number of nodes used for each parameter in different inversion cycles.

Parameters	Cycle 1	Cycle 2	Cycle 3
Temperature	4	8	10
V_{los}	1	4	4
B_z	1	3	4
B_x	0	0	0
B_y	0	0	0
Microturbulence	1	2	2

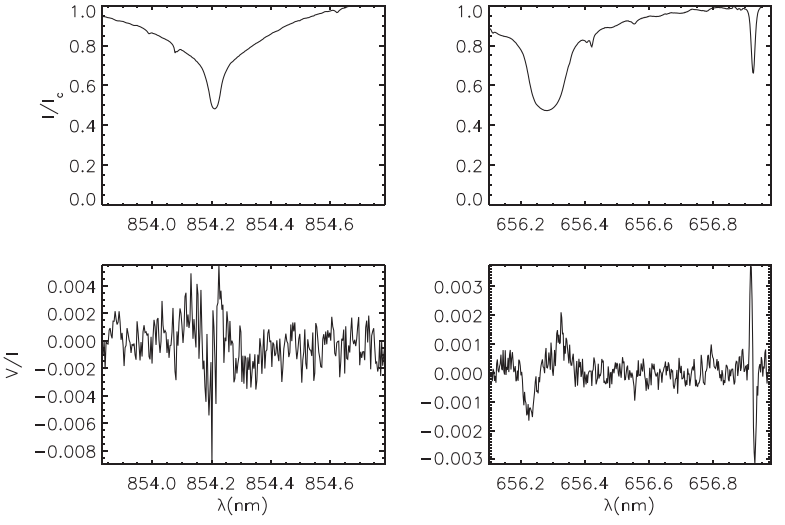

Figure 5. Stokes-I and V profiles of H α and CaIR corresponding to the region of opposite polarity (photospheric).

the photosphere. Though the signal looks very noisy, the Stokes-V of CaIR also shows the sign same as that of H α, particularly the blue-wing amplitude of the line. As seen in the raster maps of Stokes-V amplitudes as shown in Fig. 1 do not show any opposite polarity in the chromospheric lines. This suggests on the one hand that the chromospheric field that is sampled by CaIR and H α above the photospheric opposite polarity region is of canopy fields form the pore and on the other hand this observationally proves that H α indeed probes chromospheric magnetic fields.

3. Inversion CaIR Stokes-*I* and *V* profiles

Spectropolarimetric inversions of the CaIR Stokes profiles have been carried out using the NICOLE inversion code (Socas-Navarro *et al.* 2015). The inversion of quiet sun and pore profiles have been carried out in two cycles and those from SSEE region carried out in three cycles. In the first cycle lower number of nodes were used and in the next cycle the number of cycles were increased (see Table. 1). For the first cycle FALC model was used as an initial guess model. In the second cycle, the output model from the cycle-1 was used as an input guess model but with the magnetic field values replaced by those estimated through weak-field-approximation. Since, the Stokes-Q and U profiles are noise they were not considered for fitting. This was done by setting zero nodes to the horizontal components during the inversion (cf. Table. 1). Only Stokes-I and V were fitted. In the third cycle we altered the output model from cycle-2 to introduce velocity gradients. This is done only for the profiles from the region of SSEE. Signatures of velocity gradients are

https://doi.org/10.1017/S1743921320000186 Published online by Cambridge University Press

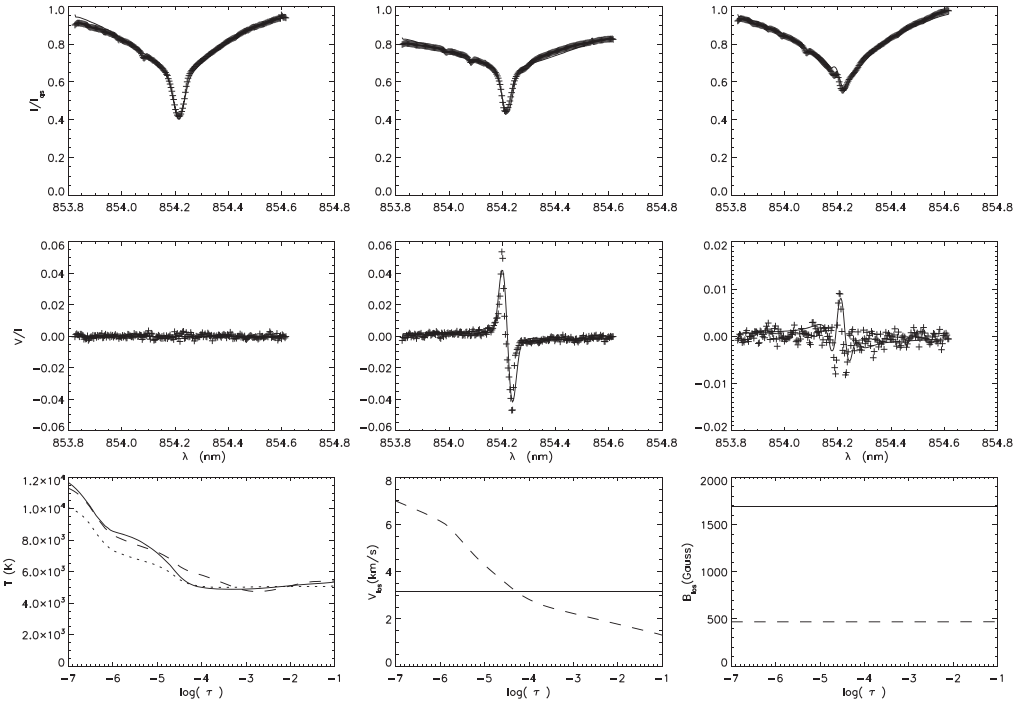

Figure 6. Plots of Stokes I (the top rows) and V (the middle rows) profiles of quiet sun (the left column), pore (the middle column) and SSEE (the right column). The observed profiles are plotted in plus symbols and the profiles fitted using NICOLE are over plotted as the solid curves. The third row shows the temperature (the left), velocity (the middle) and the LOS magnetic field (the right panel). The solid, dotted and dashed curves correspond to the quiet sun, pore and SSEE region, respectively.

clearly seen in the Stokes-I and V profiles as asymmetries. Typical observed and fitted Stokes-I (the top row) and V (the middle row) profiles are shown in Fig. 6. The panels from the left to the right in the first and the second row correspond to the regions of quiet sun, pore and SSEE. The left, the middle and the right panels in the third row show the temperature, line-of-sight (LOS) velocity and LOS magnetic field stratification (on $\log(\tau)$ scale) output from the NICOLE inversion. The solid, the dotted and the dashed curves correspond to the quiet sun, pore and SSEE regions, respectively.

The temperature derived from the inversion is lower above the pore compared to that of quiet sun except between the heihgts with $\log(\tau)$ equal to -4 and -3 where the values are comparable. The atmosphere above the pore is cooler by upto $\approx$2000 K. The temperature in the SSEE region is enhanced compared to quiet sun up to about $\approx$800 K. The maximum temperature enhancement take place close to $\log(\tau)$ equal to -4. However, the fitted profile shows the wing enhancement further away than that of observed wing enahncement (cf. the top right panel in Fig. 1) suggesting that the temperature enahcement is taking place higher up in the atmosphere than estimated by the inversion. In order to fit the profiles from SSEE regions presence velocity gradients was necessary. A typical velocity stratification from this region is shown in the middle panel of the bottom row of Fig. 6. The magnetic field output from the inversion is shown in the bottom panel of Fig. 6. Though the LOS component of the magnetic field is consistent with the observed region that field is stronger above the pore than above SSEE, there's no variation observed with height. Introduction of field gradient actually worsened the fitting of the profiles.

https://doi.org/10.1017/S1743921320000186 Published online by Cambridge University Press

4. Conclusions

Spectropolarimetric observations around a pore carried out simultaneosly in H α and CaIR have been presented. The observing period covered a small scale energetic event (SSEE). The time evolition of intensity profiles of both the lines has indicated that SSEE is a progressive reconnection event. This is produced due to an interaction between the newly emerged opposite polarity (photospheric) magnetic field and the pre-existing canopy field of the pore. Strong downflows have been observed in the beginning of this event. Comparison of intensity profiles of H α and CaIR from these downflow regions has suggested that the height of formation of CaIR may be higher than that of H α. However, more rigorous analysis is required in order to confirm this. Further, it was observed that Stokes-V profiles of H α and CaIR above opposite polarity region have sign opposite to that of photospheric lines suggesting these lines are probing the canopy fields of the pore and hence asserting that both the lines have magnetic sensitivity at the chromospheric heights. Preliminary results on the inversion of Stokes-I and V profiles of CaIR also have been presented. The atmospheric parameters derived from the inversions are consistent with the expected atmospheric conditions corresponding to different regions such as quiet sun, pore and SSEE. Further improvement in the inversions are expected which may improve the accuracy in the derived atmospheric parameters.

Acknowledgement

We would like to thank the observers at the Dunn Solar Telescope for their help in carrying out the observations presented in this paper and H. Socas-Navarro for help in setting up of NICOLE code in the initial stages.

References

Abdussamatov, H. I. 1971, *Sol. Phys*, 16, 384
Andretta, V., Jones, H. P. 1997, *ApJ*, 489, 375
Balasubramaniam, K. S., Christopoulou, E. B., Uitenbroek, H. 2004,*ApJ*, 606, 1233
Bjørgen, J. P., Leenaarts, J., Rempel, M., Cheung, M. C. M., Danilovic, S., de la Cruz Rodríguez, J., Sukhorukov, A. V. 2019, arXiv:1906.01098
Ellerman, F., 1917, *ApJ*, 46, 298
Hanaoka, Y. 2005, *Pub. Astro. Soc. Japan*, 57, 235
Kerr, G. S., Fletcher, L., Russell, A.e.J. B., Allred, J. C., 2016, *ApJ*, 827, 101
Kuridze, D., Henriques, V. M. J., Mathioudakis, M., Rouppe van der Voort, L., de la Cruz Rodríguez, J., Carlsson, M., 2018, *ApJ*, 860, 10
Lagg, A., Lites, B., Harvey, J., Gosain, S., Centeno, R., 2017, *Space Science Rev.*, 210, 37
Leenaarts, J., Carlsson, M., Rouppe van der Voort, L., 2012, *ApJ*, 749, 136
Nagaraju, K., Sankarasubramanian, K., Rangarajan, K. E., 2008, *ApJ*, 678, 531
Rutten, R. J. 2007, in Heinzel, P., Dorotovič, I., Rutten, R. J. eds, The Physics of Chromospheric Plasmas, ASP Conference Series, Volume 368, p. 27
Rutten, R. J. 2008, in Matthews, S. A., Davis, J. M., Harra, L. K., eds, First Results From Hinode, ASP Conference Series,Volume 397, p. 54
Sanchez Almeida, J., Lites, B. W., 1992, *ApJ*, 398, 359. DOI. ADS.
Schlichenmaier, R., Collados, M., 2002, *Astron. & Astrophys.*, 381, 668
Socas-Navarro, H., Uitenbroek, H., 2004, *ApJ* (letters), 603, L129
Socas-Navarro, H., Martínez Pillet, V., Elmore, D., Pietarila, A., Lites, B. W., Manso Sainz, R.m 2006, *Sol. Phys.*, 235, 75
Socas-Navarro, H., de la Cruz Rodríguez, J., Asensio Ramos, A., Trujillo Bueno, J., Ruiz Cobo, B., 2015, *Astron. & Astrophys.*, 577, 7
Vissers, G. J. M., Rouppe van der Voort, L. H. M., Rutten, R. J., Carlson, M., de Pontieu, B., 2015, *ApJ*, 812, 11